


## Resonances of Supernova Neutrinos in Twisting Magnetic Fields

Sudip Jana<sup>1,\*</sup> and Yago Porto<sup>2,†</sup>

<sup>1</sup>Max-Planck-Institut für Kernphysik, Saupfercheckweg 1, 69117 Heidelberg, Germany

<sup>2</sup>Instituto de Física Gleb Wataghin - UNICAMP, 13083-859, Campinas, São Paulo, Brazil

 (Received 28 March 2023; revised 20 June 2023; accepted 14 February 2024; published 5 March 2024)

We investigate the effect of resonant spin conversion of the neutrinos induced by the geometrical phase in a twisting magnetic field. We find that the geometrical phase originating from the rotation of the transverse magnetic field along the neutrino trajectory can trigger a resonant spin conversion of Dirac neutrinos inside the supernova, even if there were no such transitions in the fixed-direction field case. We have shown that, even though resonant spin conversion is too weak to affect solar neutrinos, it could have a remarkable consequence on supernova neutronization bursts where very intense magnetic fields are quite likely. We demonstrate how the flavor composition at Earth can be used as a probe to establish the presence of non-negligible magnetic moments, potentially down to  $10^{-15}\mu_B$  in upcoming neutrino experiments like the Deep Underground Neutrino Experiment and the Hyper-Kamiokande. Possible implications are analyzed.

DOI: 10.1103/PhysRevLett.132.101005

*Introduction.*—Pauli’s 1930 letter [1] not only postulates the neutrino’s existence as an explanation for the apparent nonconservation of energy in radioactive decay, but also suggests that these elusive particles possess a mass, along with nonzero magnetic moments. Later, in 1954, Cowan, Reines, and Harrison set the first limits on neutrino magnetic moments [2], even before neutrinos were discovered, and Bernstein, Ruderman, and Feinberg did a survey [3] of the experimental information on neutrino electromagnetic properties. In the late 1980s and early 1990s, the study of neutrino magnetic moments became a popular topic in addressing the solar neutrino problem [4–7]. In recent decades, several experiments have discovered neutrino oscillations, which conclusively demonstrated that neutrinos have masses and mixing, indicating the need for physics beyond the standard model (BSM). In such BSM theories, neutrinos establish interactions with photons via quantum loop correction, even though neutrinos are immune to electromagnetic interaction in the standard model (SM) [8]. There are now hundreds of potential neutrino mass models. Yet, not all models qualify to conceive large magnetic moments without upsetting neutrino masses (see Ref. [10] and references therein). Neutrinos with large magnetic moments can significantly impact searches at neutrino scattering experiments [11–13] and dark matter direct detection experiments [14–16], astrophysical neutrino

signals [17–22], stellar cooling [23–25], cosmological imprints [26–28], and charged lepton’s magnetic moment [29] (for a review, see Ref. [30]). The presence of large transverse magnetic fields within the Sun, supernovae, neutron stars, or other astrophysical objects can result in efficient spin precession [4,5] or resonant spin-flavor precession [6,7] of neutrinos.

The majority of the literature (see Refs. [17–22], and references therein), however, assumes that the direction of the transverse magnetic field is fixed. Nevertheless, this is not always the case. In such scenarios, neutrinos traveling from the core of the supernova outward and crossing such field configurations would encounter a transverse magnetic field whose direction changes continuously throughout their trajectory [31]. It will introduce a new geometrical phase [32] governed by the magnetic field rotation angle  $\phi$  in addition to the usual dynamical phase, determined by the energy splitting of the neutrino eigenstates. In the early 1990s, although Vidal and Wudka [34] and Aneziris and Schechter [35] discussed the effect of such phases in the context of solar neutrino problem, Smirnov was the first to correctly recognize [36] the resonant structure of neutrino spin precession due to the solar magnetic field’s geometrical phase, which was later explored by other authors [36–39]. However, we find that the impact of the geometrical phase on neutrino precession in the Sun is negligible, given a magnetic moment less than  $\sim 10^{-11}\mu_B$ , which has been ruled out by current laboratory-based experiments [13,15,16]. One needs a perhaps unrealistically large magnetic field and magnetic moment combination for an emphatic effect. Here, we have shown that it could have a remarkable consequence on supernova neutronization bursts where very intense magnetic fields are quite likely. We analyze the neutrino

---

Published by the American Physical Society under the terms of the [Creative Commons Attribution 4.0 International license](https://creativecommons.org/licenses/by/4.0/). Further distribution of this work must maintain attribution to the author(s) and the published article’s title, journal citation, and DOI. Funded by SCOAP<sup>3</sup>.

spectra from the neutronization burst phase and demonstrate how its time variation can be used as a probe to establish the presence of non-negligible magnetic moments, potentially down to  $10^{-15}\mu_B$  in forthcoming neutrino experiments like Deep Underground Neutrino Experiment (DUNE) [40] and Hyper-Kamiokande (HK) [41]. Considering a realistic setup, it will be extremely difficult to probe  $\mu_\nu \lesssim 10^{-12}\mu_B$  in laboratory-based experiments based on neutrino-electron scattering. Moreover, it has been argued that Dirac neutrino magnetic moments over  $10^{-15}\mu_B$  would not be natural [42], because they would produce unacceptable neutrino masses at larger loops. Thus, the results presented here are in the borderline of the conceivable region for  $\mu_\nu$ .

*Evolution of neutrino system in twisting magnetic field.*—Let us consider a system of left-handed neutrinos  $\nu_L = (\nu_{eL}, \nu_{\mu L}, \nu_{\tau L})$  and right-handed counterparts  $\nu_R = (\nu_{eR}, \nu_{\mu R}, \nu_{\tau R})$ , with magnetic moment  $\mu$  evolving in matter and a transverse magnetic field. If the magnetic field rotates along the neutrino path in the transverse plane, denoted by  $B = B_x + iB_y = Be^{i\phi}$ , where  $\phi(r)$  is the angle of rotation, the resulting evolution equation can be expressed as

$$i \frac{d}{dr} \begin{bmatrix} \nu_L \\ \nu_R \end{bmatrix} = \begin{bmatrix} H_L + (\dot{\phi}/2)I & \mu B(r) \\ \mu^\dagger B(r) & H_R - (\dot{\phi}/2)I \end{bmatrix} \begin{bmatrix} \nu_L \\ \nu_R \end{bmatrix}, \quad (1)$$

where  $r$  is the radial coordinate,  $I$  is the identity matrix, and  $\mu = \text{diag}\{\mu_\nu, \mu_\nu, \mu_\nu\}$  is the matrix of Dirac magnetic moments. Equation (1) is expressed in a frame [37] rotating with the magnetic field; see Fig. 1.  $H_L$  represents the Hamiltonian for  $\nu_L$  propagating in matter, given by  $H_L = (1/2E)U\Delta U^\dagger + V$ , where  $U$  is the Pontecorvo-Maki-Nakagawa-Sakata (PMNS) matrix,  $\Delta = \text{diag}\{0, \Delta m_{21}^2, \Delta m_{31}^2\}$ , and  $V = \text{diag}\{V_e, V_\mu, V_\tau\}$  is the matter potential. Assuming charge neutrality,  $V_e = \sqrt{2}G_F(n_e - 0.5n_n)$  and  $V_\mu = V_\tau = -0.5\sqrt{2}G_F n_n$ , where  $n_e$ ,  $n_p$ , and  $n_n$  are the number densities of electron, proton, and neutrons, respectively, and  $Y_e = n_e/(n_p + n_n)$  is the electron fraction.  $H_R$

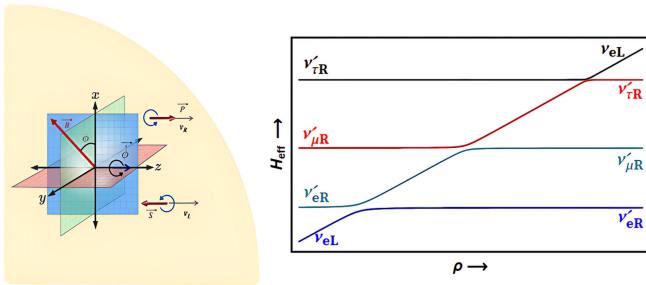


FIG. 1. Left: schematic representation of the rotating frame where the  $z$  axis denotes the direction of the neutrino momentum and  $\dot{\phi}$  is the velocity of  $B$  field rotation. The spins of  $\nu_{L,R}$  are shown by thick red arrows. Right: neutrino energy levels in the resonance region for normal ordering (NO) and  $\dot{\phi} < 0$ . See the text for details.

is the Hamiltonian for  $\nu_R$ , which does not experience matter interactions, and  $H_R = (1/2E)U\Delta U^\dagger$ . For antineutrinos,  $\bar{\nu}_L$  are the ones that do not interact with matter. Furthermore, matter potentials for antineutrinos have the opposite sign:  $\bar{V}_e = -V_e$  and  $\bar{V}_{\mu,\tau} = -V_{\mu,\tau}$ .

Now consider a neutrino system propagating in a background of the nonuniform matter and a rotating transverse magnetic field. As  $V$  changes, strong resonant spin-flip conversion,  $\nu_L \leftrightarrow \nu_R$ , can occur. In the two-state approximation, the resonance condition for the  $\nu_{\alpha L} \leftrightarrow \nu_{\alpha R}$  conversion can be expressed as [37]

$$V_\alpha + \dot{\phi} = 0. \quad (2)$$

For antineutrinos,  $\bar{\nu}_{\alpha L} \leftrightarrow \bar{\nu}_{\alpha R}$  resonance condition is  $\bar{V}_\alpha - \dot{\phi} = 0$  and occurs at the same location. The dynamics of spin-flip transition in the resonance region is governed by the adiabaticity coefficient  $\gamma_\alpha$ . Under two-state approximation, it can be expressed as [37]

$$\gamma_\alpha = \frac{2(2\mu_\nu B)^2}{|\dot{V}_\alpha + \dot{\phi}|}. \quad (3)$$

For our analysis, we study the three-flavor evolution (six states), described in Eq. (1). In such a scenario, coupled resonances (in which one resonance interferes with others owing to closeness) will exist between  $\nu_{\alpha L}$  and all  $\nu_R$  states since the right-handed (RH) states are linked among themselves as a result of mixing. The simplified neutrino energy levels in the resonance zone are depicted in Fig. 1. At high densities (to the right),  $\nu_{eL}$  is heavier than all RH states since  $V_e + \dot{\phi} (> 0)$  is very large, but the converse occurs at low densities (to the left) where  $V_e + \dot{\phi} < 0$ . The primed states in Fig. 1 are the eigenstates of  $H_R$  and, to a decent approximation, of the whole system.

*Supernova environment.*—We focus on neutrinos released during the neutronization-burst phase, which occurs right after the core bounces and lasts for a few tens of milliseconds. During this phase, the  $\nu_e$  flux is dominant over other flavors in most of the energy spectrum [17,43]. Moreover, collective neutrino oscillations, a significant source of complication to the flavor evolution, are expected to be suppressed during this stage [44,45]. The predicted neutrino fluxes during this phase have only about  $\mathcal{O}(10\%)$  uncertainty [46–49]. As a result, we anticipate that the estimates of the SN neutrino flavor content during this period are more robust.

In this work, we explore the discovery potential of the Dirac magnetic moments of neutrinos coming from SNe with magnetic field strength  $10^{10}$ – $10^{12}$  G in the iron core. Such magnetic fields are commonly associated with the formation of magnetarlike field structures in SN remnants [31]. We assume the radius of the iron core,  $r_0$ , to lie somewhere in the range of  $10^3$ – $10^4$  km (for practical calculations,  $r_0 \approx 2000$  km [31]) and model the magnetic

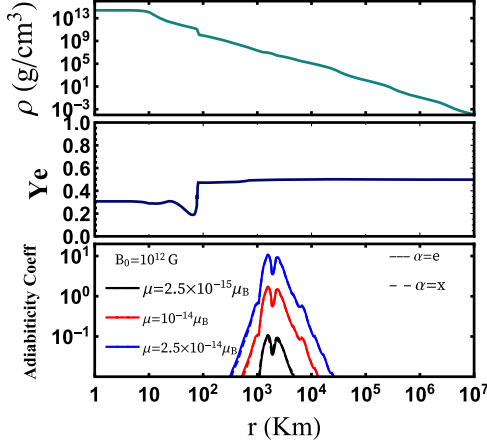


FIG. 2. Matter density  $\rho$  (upper panel), electron number fraction  $Y_e$  (middle panel), and adiabaticity coefficient  $\gamma_\alpha$  (lower panel) as a function of the radial coordinate  $r$ .

field as  $B(r) = B_0$  for  $r < r_0$  and  $B(r) = B_0(r_0/r)^3$  for  $r > r_0$  [31]. The matter potentials for  $V_e$ ,  $V_\mu$ , and  $V_\tau$  are determined by the matter density  $\rho$  and electron number fraction  $Y_e$ , which we obtain from a simulation of an  $18M_\odot$  progenitor [50] at  $t = 4.37$  ms [51]. See Fig. 2 for further details.

The spin-flip transition in the resonance region is dictated by the adiabaticity coefficient  $\gamma_\alpha$ , which is heavily influenced by  $\mu_\nu B_0$ . When taking into account the electron fraction and density of matter in the SN (cf. Fig. 2),  $\dot{V}_\alpha(r)$  varies as a function of  $r$  only, while  $\dot{\phi}(r)$  can be arbitrary. For simplicity, we assume  $|\dot{\phi}| = 0$ . This assumption is valid as long as the fluctuations around the average velocity  $\dot{\phi}$  are smaller in scale than the spin-precession scale [52], which is approximately  $\pi/\mu_\nu B_0 \sim \mathcal{O}(10)$  km at the resonance layer for  $\mu_\nu B_0 = (10^{-14}\mu_B)(10^{12}\text{ G}) = 10^{-2}\mu_B$  G. We find the surface of the iron core to be the most promising region [53] as  $\gamma_\alpha \gtrsim 1$  for values as small as  $\mu_\nu B_0 = 10^{-2}\mu_B$  G, the smallest over the whole profile. This is due to the fact that  $\rho$  decreases with  $r^{-3}$  and  $\dot{\rho}$  decreases with  $-r^{-4}$ , so  $|\dot{V}_\alpha|$  reduces as the distance ( $r$ ) from the SN center increases. At  $r = r_0$ , the smallest  $|\dot{V}_\alpha|$  occurs when the highest possible field strength,  $B(r_0) = B_0$ , is present.

At the surface of the iron core,  $Y_e \approx 0.5$  and  $n_e \approx n_n$ ; see Fig. 2. Thus, at this point,  $V_e \approx 0.5\sqrt{2}G_F n_e = -V_x$ , where  $x = \mu, \tau$ .  $V_e$  is a monotonically decreasing function in the range of  $r \sim 10^3$ – $10^4$  km, such that  $2\text{ m}^{-1} \gtrsim V_e \gtrsim 0.01\text{ m}^{-1}$ . Therefore, the rate of rotation of  $B$  in the range  $-0.01\text{ m}^{-1} \gtrsim \dot{\phi} \gtrsim -2\text{ m}^{-1}$  could produce a resonance in the  $\nu_e$  and  $\bar{\nu}_e$  channels [see Eq. (2)], while the rotation in the opposite direction  $2\text{ m}^{-1} \gtrsim \dot{\phi} \gtrsim 0.01\text{ m}^{-1}$  produces a resonance in the  $\nu_{\mu,\tau}$  and  $\bar{\nu}_{\mu,\tau}$  channels. Note that the magnitude of  $|\dot{\phi}| \sim 0.01\text{ m}^{-1}$  implies that, for resonant conversion to occur, it is sufficient for  $B$  to undergo approximately one revolution within a width of about

one kilometer (which corresponds to the resonance layer). This observation aligns with the simulation presented in [31], where the magnetic field  $B$  reverses its direction within a few kilometers around  $r_0$ .

*Analysis and results.*—Before analyzing the effect of nonzero neutrino magnetic moments, we briefly describe the signal for the standard scenario ( $\mu_\nu = 0$ ). SN neutrinos are produced at the core where  $V_e \gg V_x$  and the electron neutrino ( $\nu_e$ ) becomes the heaviest of the three matter eigenstates, either as  $\nu_{3m}$  for normal mass ordering (NO) or as  $\nu_{2m}$  for inverted mass ordering (IO); while the muon neutrino ( $\nu_\mu$ ) and tau neutrino ( $\nu_\tau$ ) are a combination of the two remaining eigenstates. The opposite is true for anti-neutrinos, where the electron antineutrino ( $\bar{\nu}_e$ ) becomes the lightest of the three eigenstates in matter, either as  $\bar{\nu}_{1m}$  in NO or as  $\bar{\nu}_{3m}$  in IO, because  $\bar{V}_e \ll \bar{V}_x$ . During the subsequent evolution, neutrinos and antineutrinos might cross adiabatically the low ( $L$ ) and high ( $H$ ) Mikheyev-Smirnov-Wolfenstein resonances [55–57]. These happen when  $|V_e - V_x| = |\Delta m_{n1}^2| \cos \theta_{1n}/2E$ , where  $n = 2$  ( $n = 3$ ) for  $L$  ( $H$ ) resonance. In NO,  $L$  and  $H$  resonances occur exclusively in the neutrino channel, but in IO,  $L$  resonance occurs for neutrinos and  $H$  resonance for antineutrinos [58]. Considering the best-fit values for the oscillation parameters [59],  $H$  resonance occurs at about  $3 \times 10^4$  km, whereas  $L$  resonance occurs at approximately  $2 \times 10^5$  km from the center of the SN. In NO, at the production region  $\nu_e \approx \nu_{3m}$ , so  $\Phi_{i3} = \Phi_{ie}$ . At vacuum, however, only a small component of  $\nu_3$ ,  $|U_{e3}| \approx 0.02$ , remains as electron flavor. Therefore, only  $0.02\Phi_{ie}$  contributes to the final  $\nu_e$  flux. Assuming the initial  $\nu_\mu$  flux and  $\nu_\tau$  flux to be equal,  $\Phi_{i\mu} = \Phi_{i\tau} = \Phi_{ix}$ , the initial fluxes of the remaining matter eigenstates  $\nu_{1m}$  and  $\nu_{2m}$ , which are mixtures of  $\nu_\mu$  and  $\nu_\tau$ , are also equal to  $\Phi_{ix}$ . Thus, their respective contributions to the final  $\nu_e$  flux are  $|U_{e1}|^2\Phi_{ix}$  and  $|U_{e2}|^2\Phi_{ix}$ . The total final  $\nu_e$  flux in NO is then

$$\Phi_e^{\text{NO}} = |U_{e3}|^2\Phi_{ie} + (1 - |U_{e3}|^2)\Phi_{ix} \approx 0.02\Phi_{ie} + 0.98\Phi_{ix}, \quad (4)$$

where we used the unitarity of the PMNS matrix to write  $|U_{e1}|^2 + |U_{e2}|^2 = 1 - |U_{e3}|^2$ . Similarly, for IO:  $\Phi_{i2} = \Phi_{ie}$ , while  $\Phi_{i1} = \Phi_{i3} = \Phi_{ix}$ ; therefore,

$$\Phi_e^{\text{IO}} = |U_{e2}|^2\Phi_{ie} + (1 - |U_{e2}|^2)\Phi_{ix} \approx 0.3\Phi_{ie} + 0.7\Phi_{ix}. \quad (5)$$

For antineutrinos, at the production point,  $\bar{\nu}_e \approx \bar{\nu}_{1m}$  in NO and  $\bar{\nu}_e \approx \bar{\nu}_{3m}$  in IO. Then, we have

$$\Phi_{\bar{e}}^{\text{NO}} = |U_{e1}|^2\Phi_{i\bar{e}} + (1 - |U_{e1}|^2)\Phi_{ix} \approx 0.7\Phi_{i\bar{e}} + 0.3\Phi_{ix}, \quad (6)$$

$$\Phi_{\bar{e}}^{\text{IO}} = |U_{e3}|^2\Phi_{i\bar{e}} + (1 - |U_{e3}|^2)\Phi_{ix} \approx 0.02\Phi_{i\bar{e}} + 0.98\Phi_{ix}. \quad (7)$$

Now we analyze the effect of the new resonance due to twisting magnetic fields at the surface of the SN iron core. This resonance can happen at  $r \sim r_0$ , before the  $L$  and  $H$  resonances take place, and can have profound consequences to the fluxes [see Eqs. (4)–(7)], coming out of the collapsing star during the neutronization-burst phase. The reason is that a sizable fraction of active neutrinos could be converted to their right-handed counterparts, effectively decreasing the initial fluxes before they reach the  $L$  and  $H$  resonances, i.e.,

$$\Phi_{i\alpha} \rightarrow e^{-(\pi/2)\gamma_\alpha} \Phi_{i\alpha}, \quad (8)$$

for the specific flavor  $\alpha$  which has the resonance condition in Eq. (2) satisfied. The Landau-Zener factor  $e^{-(\pi/2)\gamma_\alpha}$  is the “flip” probability that a transition happens between the states  $\nu_{\alpha L} \leftrightarrow \nu_{\alpha R}$  at the resonance point. In what follows, we analyze the limiting case of total adiabaticity, where  $\gamma_\alpha > 1$ . Indeed, Fig. 2 shows that, for  $\mu_\nu B_0 = (10^{-14} \mu_B)(10^{12} \text{ G}) = 10^{-2} \mu_B \text{ G}$ ,  $\gamma_\alpha \approx 2$  and  $e^{-(\pi/2)\gamma_\alpha} \approx 0.04$  in specific locations, resulting in dramatic modifications to the expected neutronization fluxes.

We obtain the initial neutrino fluxes from a spherically symmetric  $15M_\odot$  progenitor simulation [60] and consider the time interval between  $-5$  and  $40$  ms as corresponding to the neutronization-burst phase. We separate the detected signal in two periods:  $-5 \text{ ms} < t < 20 \text{ ms}$ , that encompasses the neutronization peak [17,43] and has initial fluxes that are roughly related by  $\Phi_{ie} \approx 10\Phi_{ix}$  and  $\Phi_{ix} \approx 10\Phi_{i\bar{e}}$ , and  $20 \text{ ms} < t < 40 \text{ ms}$ , which has initial fluxes  $\Phi_{ie} \approx \Phi_{i\bar{e}} \approx \Phi_{ix}$ . Here, we compute the percentage reduction for the neutronization-burst fluxes relative to the expectation described by Eqs. (4)–(7) if the spin-flip resonance is crossed adiabatically. (1) For  $-0.01 \text{ m}^{-1} \gtrsim \dot{\phi} \gtrsim -2 \text{ m}^{-1}$ , the resonance would lie in the  $\nu_e$  and  $\bar{\nu}_e$  channels. We can account for the effect by making  $\Phi_{ie} \rightarrow 0$  in (4) and (5) while  $\Phi_{i\bar{e}} \rightarrow 0$  in (6) and (7): (a)  $t < 20 \text{ ms}$ —reduction of 17% for  $\Phi_e^{\text{NO}}$ , 81% for  $\Phi_e^{\text{IO}}$ , 19% for  $\Phi_{\bar{e}}^{\text{NO}}$ , and 0% for  $\Phi_{\bar{e}}^{\text{IO}}$ ; (b)  $t < 20 \text{ ms}$ —reduction of 2% for  $\Phi_e^{\text{NO}}$ , 30% for  $\Phi_e^{\text{IO}}$ , 70% for  $\Phi_{\bar{e}}^{\text{NO}}$ , and 2% for  $\Phi_{\bar{e}}^{\text{IO}}$ . (2) For  $2 \text{ m}^{-1} \gtrsim \dot{\phi} \gtrsim 0.01 \text{ m}^{-1}$ , there could be a resonance in the  $\nu_{\mu,\tau}$  and  $\bar{\nu}_{\mu,\tau}$  channels. The consequence is that  $\Phi_{ix} \rightarrow 0$  in all Equations from (4) to (7): (a)  $t < 20 \text{ ms}$ —reduction of 83% for  $\Phi_e^{\text{NO}}$ , 19% for  $\Phi_e^{\text{IO}}$ , 81% for  $\Phi_{\bar{e}}^{\text{NO}}$ , and 100% for  $\Phi_{\bar{e}}^{\text{IO}}$ ; (b)  $t < 20 \text{ ms}$ —reduction of 98% for  $\Phi_e^{\text{NO}}$ , 70% for  $\Phi_e^{\text{IO}}$ , 30% for  $\Phi_{\bar{e}}^{\text{NO}}$ , and 98% for  $\Phi_{\bar{e}}^{\text{IO}}$ . These numbers indicate that twisting magnetic fields can impact the time variation of the neutronization-burst signal. In particular, case 1 optimizes the impact of the new resonance for inverted ordering (IO), resulting in up to an 81% reduction in the  $\nu_e$  neutronization peak, which occurs before 20 ms and is significant in the standard case for IO; see the difference between the green and red lines in the panel for DUNE, IO in Fig. 3. However, case 2 has the highest

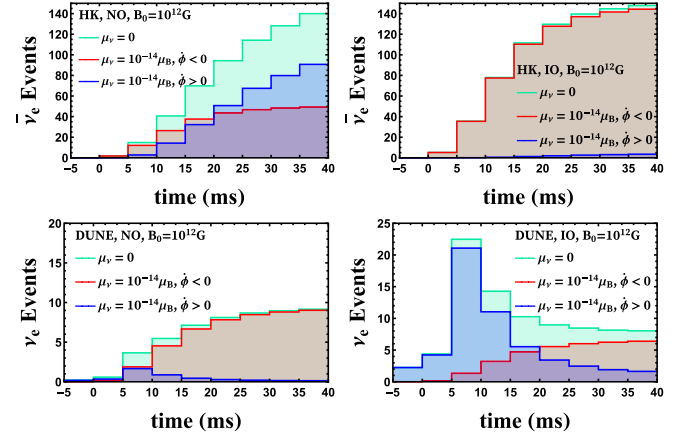


FIG. 3. Expected number of  $\bar{\nu}_e$  events at HK (upper) and  $\nu_e$  events at DUNE (lower) for NO (left) and IO (right) in the time window between  $-5$  and  $40$  ms corresponding to the SN neutronization-burst stage in which  $0$  ms is the time of core bounce. Results are shown for the standard scenario ( $\mu_\nu = 0$ ) and for  $\mu_\nu = 10^{-14} \mu_B$  and  $B_0 = 10^{12} \text{ G}$  for both cases 1 ( $\dot{\phi} < 0$ ) and 2 ( $\dot{\phi} > 0$ ).

potential for demonstrating the effects of twisting magnetic fields, since it can cause a strong suppression (greater than 70%) of neutrino fluxes in almost every detection channel and time window.

Figure 3 depicts cases 1 ( $\dot{\phi} = -0.9 \text{ m}^{-1}$ ) and 2 ( $\dot{\phi} = +0.9 \text{ m}^{-1}$ ) in future experiments like DUNE [40], a 40 kt liquid argon time-projection chamber, which mainly detects  $\nu_e$  via  $\nu_e + {}^{40}\text{Ar} \rightarrow {}^{40}\text{K}^* + e^-$ , and HK [41], a 374 kt water-Cherenkov detector, which detects mainly  $\bar{\nu}_e$  via inverse-beta decay,  $\bar{\nu}_e + p \rightarrow e^+ + n$ . The number of detected events of  $\nu_\alpha$  per energy is

$$\frac{dN_{\nu_\alpha}}{dE_r} = \frac{N_t}{4\pi R^2} \int dE_t \Phi_\alpha(E_t) \sigma_\alpha(E_t) W(E_r, E_t), \quad (9)$$

where  $N_t$  denotes the number of target particles in the detector,  $R = 10 \text{ kpc}$  is the distance between Earth and the galactic SN,  $\Phi_\alpha$  and  $\sigma_\alpha$  represent  $\nu_\alpha$  flux and interaction cross section, respectively, and  $W$  is the energy-resolution function. For technical details, see Ref. [17]. To study the sensitivity of DUNE and HK to a nonzero  $\mu_\nu$  in the presence of resonant spin-precession, we use the  $\chi^2$  estimator

$$\chi^2 = \min_{\xi} \sum_{i=1}^n 2 \left[ (1 + \xi) F_i - D_i + D_i \ln \left( \frac{D_i}{(1 + \xi) F_i} \right) \right], \quad (10)$$

with  $F_i$  and  $D_i$  the number of events in the  $i$ th time bin for finite and null values of  $\mu_\nu$ , respectively. We perform a shape-only analysis where the normalization parameter  $\xi$  varies in the range  $[-1, 1000]$  and adjust the normalization

TABLE I. Experimental sensitivities on  $\mu_\nu$  for different benchmark scenarios and  $B_0 = 10^{12}$  G.

Experiments	Discovery reach for $\mu_\nu$ (in $\mu_B$ )			
	$\dot{\phi} < 0$		$\dot{\phi} > 0$	
	NO	IO	NO	IO
HK	$8 \times 10^{-15}$	...	$8 \times 10^{-15}$	$4 \times 10^{-15}$
DUNE	...	$7.2 \times 10^{-15}$	$1 \times 10^{-14}$	$8.2 \times 10^{-15}$
DUNE + HK	$7.5 \times 10^{-15}$	$7.2 \times 10^{-15}$	$7 \times 10^{-15}$	$4 \times 10^{-15}$

of the test hypothesis to the true hypothesis. In this way, the analysis concentrates on the time variation of the signal. Discovery reaches for DUNE and HK, as well as the combined analysis of both experiments, are summarized in Table I. The sensitivity of the combination of DUNE and HK can reach  $\mu_\nu$  of the order of  $4 - 7.5 \times 10^{-15} \mu_B$  at 90% C.L. for  $B_0 = 10^{12}$  G [61].

Interstellar magnetic fields influence only the overall flux normalization [19] and not its temporal variation. Hence, if supernova flux is measured in the future and the flux deficit is seen to be different in various time bins, this will occur owing to the above-mentioned resonances caused by the magnetic field configuration's twisting structure. While the intriguing effect could appear in the observed (anti)neutrino spectra at HK and DUNE experiments, the reality is expected to be significantly more intricate, necessitating future research. Even with assumed knowledge of neutrinos as Dirac fermions and known mass ordering, uncontrollable factors, including other BSM effects, may influence the magnetic moment effect.

*Final remarks.*—We have shown that if the magnetic field inside the supernova has a twisting structure, then the rotation of the magnetic field along the neutrino trajectory can induce a resonant spin conversion, which will affect predictions for the event rates when detecting supernova neutrinos in future neutrino experiments such as DUNE and HK. If neutrinos are Dirac particles possessing large magnetic moments, this resonance effect will present the optimal avenue toward unraveling the scenario at hand.

We thank Alexei Y. Smirnov for useful discussions.

\* sudip.jana@mpi-hd.mpg.de

† yporto@ifi.unicamp.br

- [1] W. Pauli, Dear radioactive ladies and gentlemen, *Phys. Today* **31N9**, 27 (1978), <https://inspirehep.net/literature/45177>.
- [2] C. L. Cowan, F. Reines, and F. B. Harrison, Upper limit on the neutrino magnetic moment, *Phys. Rev.* **96**, 1294 (1954).
- [3] J. Bernstein, M. Ruderman, and G. Feinberg, Electromagnetic properties of the neutrino, *Phys. Rev.* **132**, 1227 (1963).

- [4] A. Cisneros, Effect of neutrino magnetic moment on solar neutrino observations, *Astrophys. Space Sci.* **10**, 87 (1971).
- [5] L. B. Okun, M. B. Voloshin, and M. I. Vysotsky, Neutrino electrodynamics and possible effects for solar neutrinos, *Sov. Phys. JETP* **64**, 446 (1986), <https://inspirehep.net/literature/229944>.
- [6] C.-S. Lim and W. J. Marciano, Resonant spin—flavor precession of solar and supernova neutrinos, *Phys. Rev. D* **37**, 1368 (1988).
- [7] E. K. Akhmedov, Resonant amplification of neutrino spin rotation in matter and the solar neutrino problem, *Phys. Lett. B* **213**, 64 (1988).
- [8] In the SM, the chiral symmetry obeyed by massless neutrinos demands  $\mu_\nu = 0$ . In the minimal SM +  $\nu_R$  scenario,  $\mu_\nu$  is expected to be  $\mu_\nu = (eG_F m_\nu / 8\sqrt{2}\pi^2) = 3 \times 10^{-20} \mu_B (m_\nu / 0.1 \text{ eV})$  [9].
- [9] K. Fujikawa and R. E. Shrock, The magnetic moment of a massive neutrino and neutrino spin rotation, *Phys. Rev. Lett.* **45**, 963 (1980).
- [10] K. S. Babu, S. Jana, and M. Lindner, Large neutrino magnetic moments in the light of recent experiments, *J. High Energy Phys.* **10** (2020) 040.
- [11] A. G. Beda, V. B. Brudanin, V. G. Egorov, D. V. Medvedev, V. S. Pogosov, M. V. Shirchenko, and A. S. Starostin, The results of search for the neutrino magnetic moment in GEMMA experiment, *Adv. High Energy Phys.* **2012**, 350150 (2012).
- [12] M. Agostini *et al.* (Borexino Collaboration), Limiting neutrino magnetic moments with Borexino Phase-II solar neutrino data, *Phys. Rev. D* **96**, 091103 (2017).
- [13] H. Bonet *et al.* (CONUS Collaboration), First upper limits on neutrino electromagnetic properties from the CONUS experiment, *Eur. Phys. J. C* **82**, 813 (2022).
- [14] E. Aprile *et al.* (XENON Collaboration), Excess electronic recoil events in XENON1T, *Phys. Rev. D* **102**, 072004 (2020).
- [15] E. Aprile *et al.* (XENON Collaboration), Search for new physics in electronic recoil data from XENONnT, *Phys. Rev. Lett.* **129**, 161805 (2022).
- [16] J. Aalbers *et al.* (LZ Collaboration), First dark matter search results from the LUX-ZEPLIN (LZ) experiment, *Phys. Rev. Lett.* **131**, 041002 (2023).
- [17] S. Jana, Y. P. Porto-Silva, and M. Sen, Exploiting a future galactic supernova to probe neutrino magnetic moments, *J. Cosmol. Astropart. Phys.* **09** (2022) 079.
- [18] E. Akhmedov and P. Martínez-Miravé, Solar  $\bar{\nu}_e$  flux: Revisiting bounds on neutrino magnetic moments and solar magnetic field, *J. High Energy Phys.* **10** (2022) 144.
- [19] J. Kopp, T. Opferkuch, and E. Wang, Magnetic moments of astrophysical neutrinos, [arXiv:2212.11287](https://arxiv.org/abs/2212.11287).
- [20] S. Ando and K. Sato, Three generation study of neutrino spin flavor conversion in supernova and implication for neutrino magnetic moment, *Phys. Rev. D* **67**, 023004 (2003).
- [21] A. Ahriche and J. Mimouni, Supernova neutrino spectrum with matter and spin flavor precession effects, *J. Cosmol. Astropart. Phys.* **11** (2003) 004.
- [22] E. K. Akhmedov and T. Fukuyama, Supernova prompt neutronization neutrinos and neutrino magnetic moments, *J. Cosmol. Astropart. Phys.* **12** (2003) 007.

- [23] N. Viaux, M. Catelan, P. B. Stetson, G. G. Raffelt, J. Redondo, A. A. R. Valcarce, and A. Weiss, Neutrino and axion bounds from the globular cluster M5 (NGC 5904), *Phys. Rev. Lett.* **111**, 231301 (2013).
- [24] N. Viaux, M. Catelan, P. B. Stetson, G. Raffelt, J. Redondo, A. A. R. Valcarce, and A. Weiss, Particle-physics constraints from the globular cluster M5: Neutrino Dipole Moments, *Astron. Astrophys.* **558**, A12 (2013).
- [25] F. Capozzi and G. Raffelt, Axion and neutrino bounds improved with new calibrations of the tip of the red-giant branch using geometric distance determinations, *Phys. Rev. D* **102**, 083007 (2020).
- [26] N. Vassh, E. Grohs, A. B. Balantekin, and G. M. Fuller, Majorana neutrino magnetic moment and neutrino decoupling in big bang nucleosynthesis, *Phys. Rev. D* **92**, 125020 (2015).
- [27] S.-P. Li and X.-J. Xu, Neutrino magnetic moments meet precision  $N_{\text{eff}}$  measurements, *J. High Energy Phys.* **02** (2023) 085.
- [28] E. Grohs and A. B. Balantekin, Implications on cosmology from dirac neutrino magnetic moments, *Phys. Rev. D* **107**, 123502 (2023).
- [29] K. S. Babu, S. Jana, M. Lindner, and V. P. K., Muon  $g - 2$  anomaly and neutrino magnetic moments, *J. High Energy Phys.* **10** (2021) 240.
- [30] C. Giunti and A. Studenikin, Neutrino electromagnetic interactions: A window to new physics, *Rev. Mod. Phys.* **87**, 531 (2015).
- [31] M. Bugli, J. Guilet, M. Obergaulinger, P. Cerdá-Durán, and M. A. Aloy, The impact of non-dipolar magnetic fields in core-collapse supernovae, *Mon. Not. R. Astron. Soc.* **492**, 58 (2020).
- [32] The Berry phase [33] arises from the time dependency of parameters entering the Hamiltonian of a quantum system.
- [33] M. V. Berry, Quantal phase factors accompanying adiabatic changes, *Proc. R. Soc. A* **392**, 45 (1984).
- [34] J. Vidal and J. Wudka, Nondynamical contributions to left-right transitions in the solar neutrino problem, *Phys. Lett. B* **249**, 473 (1990).
- [35] C. Aneziris and J. Schechter, Neutrino 'spin rotation' in a twisting magnetic field, *Int. J. Mod. Phys. A* **06**, 2375 (1991).
- [36] A. Y. Smirnov, The geometrical phase in neutrino spin precession and the solar neutrino problem, *Phys. Lett. B* **260**, 161 (1991).
- [37] E. K. Akhmedov, A. Y. Smirnov, and P. I. Krastev, Resonant neutrino spin flip transitions in twisting magnetic fields, *Z. Phys. C* **52**, 701 (1991).
- [38] E. K. Akhmedov, S. T. Petcov, and A. Y. Smirnov, Pontecorvo's original oscillations revisited, *Phys. Lett. B* **309**, 95 (1993).
- [39] A. B. Balantekin and F. Loreti, Consequences of twisting solar magnetic fields in solar neutrino experiments, *Phys. Rev. D* **48**, 5496 (1993).
- [40] B. Abi *et al.* (DUNE Collaboration), Supernova neutrino burst detection with the deep underground neutrino experiment, *Eur. Phys. J. C* **81**, 423 (2021).
- [41] K. Abe *et al.* (Hyper-Kamiokande Collaboration), Supernova model discrimination with Hyper-Kamiokande, *Astrophys. J.* **916**, 15 (2021).
- [42] N. F. Bell, V. Cirigliano, M. J. Ramsey-Musolf, P. Vogel, and M. B. Wise, How magnetic is the Dirac neutrino?, *Phys. Rev. Lett.* **95**, 151802 (2005).
- [43] A. de Gouvêa, I. Martínez-Soler, and M. Sen, Impact of neutrino decays on the supernova neutronization-burst flux, *Phys. Rev. D* **101**, 043013 (2020).
- [44] A. de Gouvea and S. Shalgar, Effect of transition magnetic moments on collective supernova neutrino oscillations, *J. Cosmol. Astropart. Phys.* **10** (2012) 027.
- [45] A. Mirizzi, I. Tamborra, H.-T. Janka, N. Saviano, K. Scholberg, R. Bollig, L. Hudepohl, and S. Chakraborty, Supernova neutrinos: Production, oscillations and detection, *Riv. Nuovo Cimento* **39**, 1 (2016).
- [46] P. D. Serpico, S. Chakraborty, T. Fischer, L. Hudepohl, H.-T. Janka, and A. Mirizzi, Probing the neutrino mass hierarchy with the rise time of a supernova burst, *Phys. Rev. D* **85**, 085031 (2012).
- [47] J. Wallace, A. Burrows, and J. C. Dolence, Detecting the supernova breakout burst in terrestrial neutrino detectors, *Astrophys. J.* **817**, 182 (2016).
- [48] E. O'Connor *et al.*, Global comparison of core-collapse supernova simulations in spherical symmetry, *J. Phys. G* **45**, 104001 (2018).
- [49] M. Kachelriess, R. Tomas, R. Buras, H. T. Janka, A. Marek, and M. Rampp, Exploiting the neutronization burst of a galactic supernova, *Phys. Rev. D* **71**, 063003 (2005).
- [50] T. Fischer, S. C. Whitehouse, A. Mezzacappa, F. K. Thielemann, and M. Liebendorfer, Protoneutron star evolution and the neutrino driven wind in general relativistic neutrino radiation hydrodynamics simulations, *Astron. Astrophys.* **517**, A80 (2010).
- [51] J. Tang, T. Wang, and M.-R. Wu, Constraining sterile neutrinos by core-collapse supernovae with multiple detectors, *J. Cosmol. Astropart. Phys.* **10** (2020) 038.
- [52] P. I. Krastev and A. Y. Smirnov, Parametric effects in neutrino oscillations, *Phys. Lett. B* **226**, 341 (1989).
- [53] Note that the resonance criterion [cf. Eq. (2)] cannot be achieved for  $\dot{\phi} = 0$  outside the region where neutrinos are produced,  $r \gtrsim 100$  km [54], and, even when satisfied for  $r \lesssim 100$  km, it cannot be adiabatic unless considering unrealistically large magnetic moment and magnetic field combination.
- [54] H. T. Janka, Neutrino emission from supernovae, *Handbook of Supernovae* (Springer, Cham, 2017).
- [55] L. Wolfenstein, Neutrino oscillations in matter, *Phys. Rev. D* **17**, 2369 (1978).
- [56] S. P. Mikheyev and A. Y. Smirnov, Resonance amplification of oscillations in matter and spectroscopy of solar neutrinos, *Sov. J. Nucl. Phys.* **42**, 913 (1985), <https://inspirehep.net/literature/228623>.
- [57] S. P. Mikheev and A. Y. Smirnov, Neutrino oscillations in an inhomogeneous medium: Adiabatic regime, *Sov. Phys. JETP* **65**, 230 (1987), <https://inspirehep.net/literature/254687>.
- [58] A. S. Dighe and A. Y. Smirnov, Identifying the neutrino mass spectrum from the neutrino burst from a supernova, *Phys. Rev. D* **62**, 033007 (2000).
- [59] P. F. de Salas, D. V. Forero, S. Gariazzo, P. Martínez-Miravé, O. Mena, C. A. Ternes, M. Tórtola, and J. W. F. Valle, 2020

global reassessment of the neutrino oscillation picture, *J. High Energy Phys.* **02** (2021) 071.

[60] Garching core-collapse supernova archive, <https://www.mpa-garching.mpg.de/ccsnarchive/>.

[61] However, larger magnetic fields, up to  $10^{16}$  G [62], are possible in neutron star mergers, and the interplay of matter effects in the merger ejecta and twisting magnetic fields could

impact the perceived initial flavor-ratios coming from these sources.

[62] C. Palenzuela, R. Aguilera-Miret, F. Carrasco, R. Ciolfi, J. V. Kalinani, W. Kastaun, B. Miñano, and D. Viganò, Turbulent magnetic field amplification in binary neutron star mergers, *Phys. Rev. D* **106**, 023013 (2022).